GEOS F493 / F693
Geodetic Methods and Modeling

– Lecture 02: Instrumentation overview–

Ronni Grapenthin
rgrapenthin@alaska.edu
Elvey 413B
(907) 474-7286

September 09, 2019

Geodesy

Geodesy is the study of the size, shape and gravity field of the Earth and Earth's orientation in space.

Some (modern) techniques

- Global Navigation Satellite System (GNSS, includes GPS)
- Interferometric Synthetic Aperture Radar Analysis (space-based, ground-based)
- Electronic Tiltmeters
- Gravity Measurements (space, ground)
- Electronic Distance Measurement (EDM)
- Laser Scanning (LiDAR; terrestrial, aerial)
- Structure from Motion (SfM)

GNSS - Continuous Installations 1/3

short-term continuous:

Picture: R. Grapenthin

GNSS - Continuous Installations 2/3

very stable:

Picture: UNAVCO

GNSS - Continuous Installations 3/3

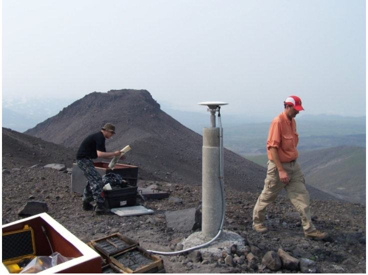

GNSS - Campaign / Episodic Installations 1/5

Benchmark:

images: R. Grapenthin

GNSS - Campaign / Episodic Installations 2/5

Benchmark:

images: R. Grapenthin

GNSS - Campaign / Episodic Installations 3/5

Setup (spike mount):

images: R. Grapenthin

GNSS - Campaign / Episodic Installations 4/5

Setup (tripod):

images: R. Grapenthin

GNSS - Campaign / Episodic Installations 5/5

Setup (tripod):

images: R. Grapenthin

GNSS - Products: time series

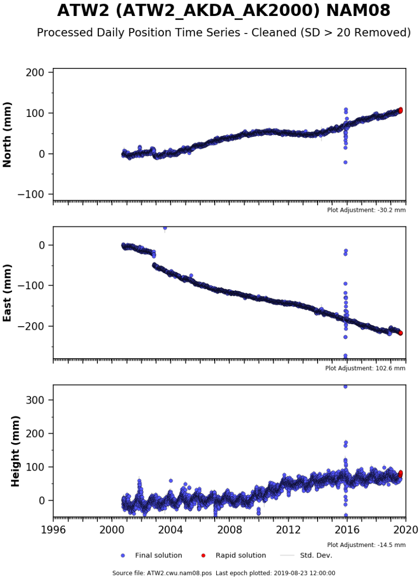

UNAVCO

GNSS - Products: Displacement Maps

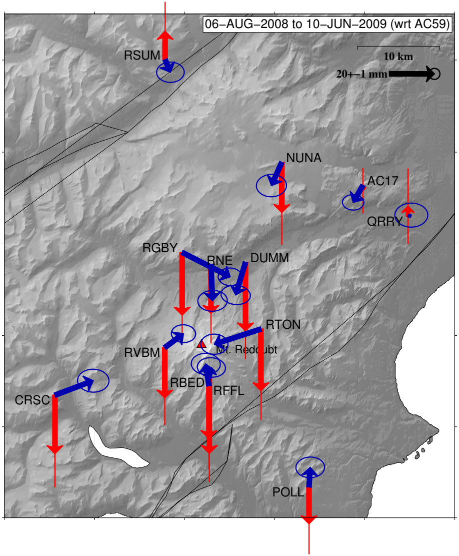

Grapenthin et al., 2013

GNSS - Products: velocity fields

Herring et al.. 2018

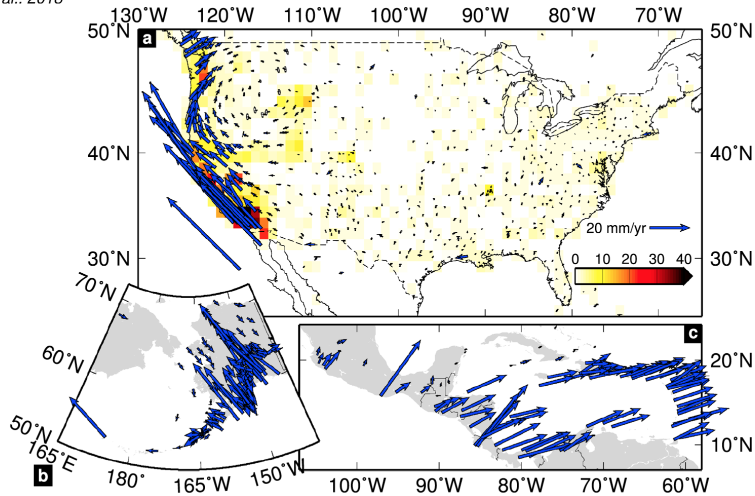

Figure 1. Horizontal velocities from the GAGE solution in (a) the contiguous United States, (b) Alaska, and (c) the Caribbean. The solution is decimated for clarity in Figure 1a, where only approximately 15% of the stations in the solution are shown west of 110°W. Velocity uncertainties are plotted at 95% confidence but are imperceptibly small at this scale. The background color map in Figure 1a shows the station density per square degree of the processed network in the contiguous U.S.

InSAR - space-based

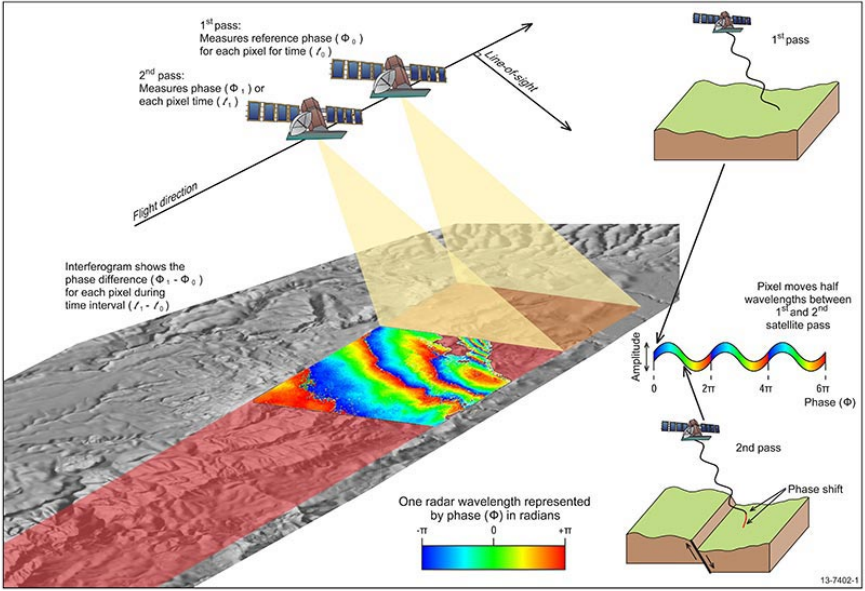

source: Geoscience Australia, http://www.ga.gov.au/scientific-topics/positioning-navigation/geodesy/geodetic-techniques/interferometric-synthetic-aperture-radar

InSAR - Products: Interferograms

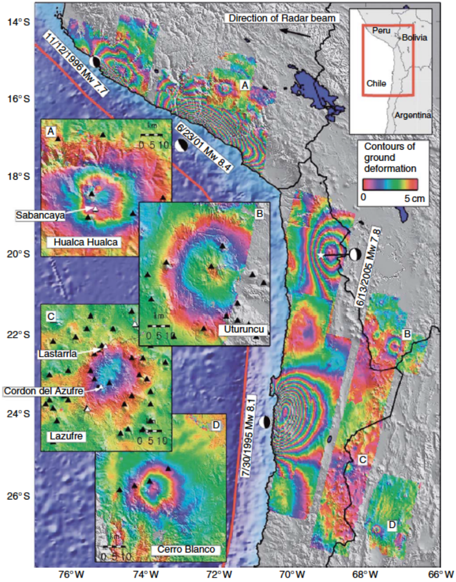

Simons and Rosen, 2007

InSAR - Products: Time Series

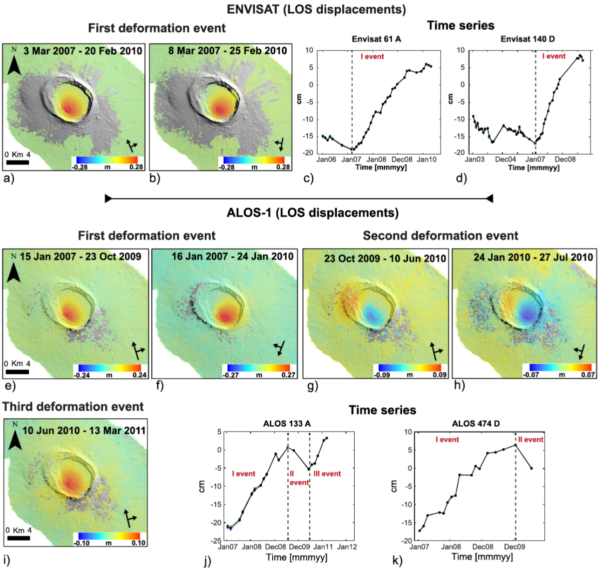

Figure 2. Time series results. ENVISAT LOS displacement map (a) for ascending orbit 61 (March 2007 to February 2010) and (b) for descending orbit 140 (March 2007 to February 2010). (c and d) ENVISAT time series (ts) (see star in Figure 1c for location). ALOS-1 LOS displacement map (e) for ascending orbit 133 (January 2007 to October 2009) and (f) for descending orbit 474 (January 2007 to January 2010). ALOS-1 LOS displacement map (g) for ascending orbit 133 (October 2009 to June 201) and (h) for descending orbit 474 (January 2010 to July 2010). (i) ALOS-1 LOS displacement map for ascending orbit 133 (June 2010 to March 2011). (j and k) ALOS-1 time series (see star in Figure 1c for location). In (a), (b), and (e)–(i) data are unwrapped, and spatially correlated look-angle errors

Ground-based SAR 1/2

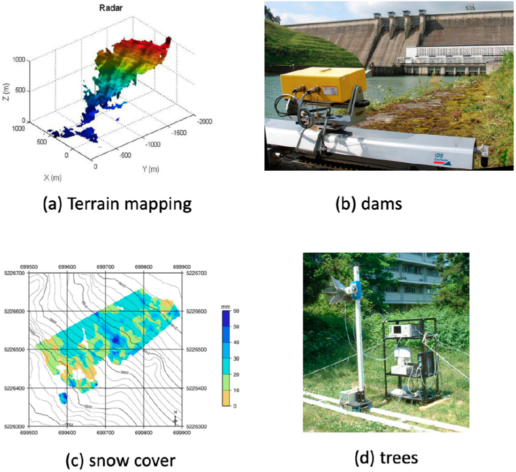

Figure 11. Examples of GBRI applications: (**a**) terrain mapping, digital elevation model of a slope obtained through GBSAR (after [84]) (**b**) dams monitoring (courtesy of IDS georadar [48]); (**c**) snow cover monitoring, map of snow water equivalent change obtained by GBSAR (after [85]); (**d**) trees monitoring by GBSAR (after [86]).

source: Pieraccini and Miccinesi, 2019, Remote Sensing

Ground-based SAR 2/2

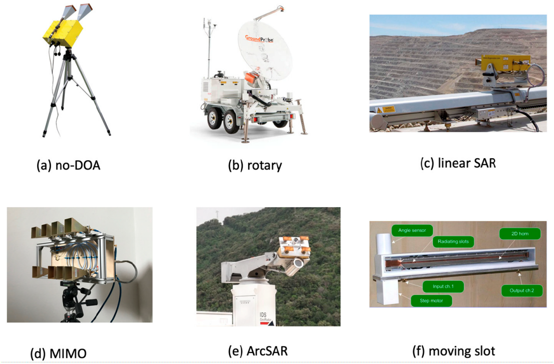

Figure 4. Examples of ground-based radar interferometers: (**a**) no-DOA (after [48]); (**b**) Rotary (after [49]); (**c**) linear SAR (after [48]); (**d**) MIMO (after [50]); (**e**) ArcSAR (after [48]); (**f**) moving slot (after [21]).

source: Pieraccini and Miccinesi, 2019, Remote Sensing

Tiltmeters: Florida Installation - Borehole

Tiltmeters: Florida Installation - Borehole

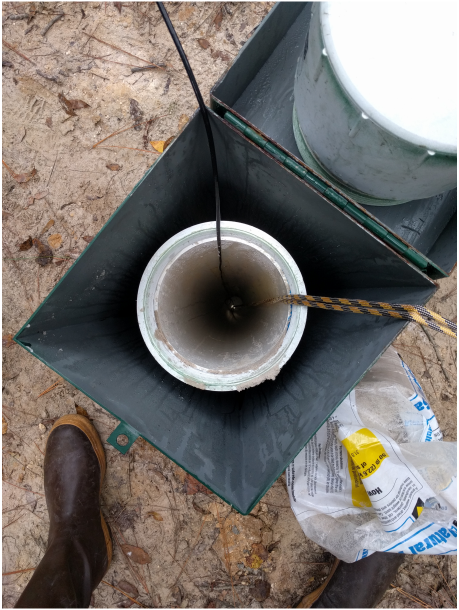

Tiltmeters: Florida Installation - Borehole

Tiltmeters: Florida Installation - Borehole

Tiltmeters: Florida Installation - Borehole

R. Grapenthin

Tiltmeters: Florida Installation - Borehole

Tiltmeters: Florida Installation - Borehole

R. Grapenthin

Tiltmeters: Florida Installation - Borehole

R. Grapenthin

Tiltmeters: Florida Installation - Platform

R. Grapenthin

Tiltmeters: Florida Installation - Platform

Tiltmeters: Florida Installation - Platform

R. Grapenthin

Tiltmeters: Florida Installation - Platform

R. Grapenthin

Tiltmeters: Florida Installation - Platform

Tiltmeters

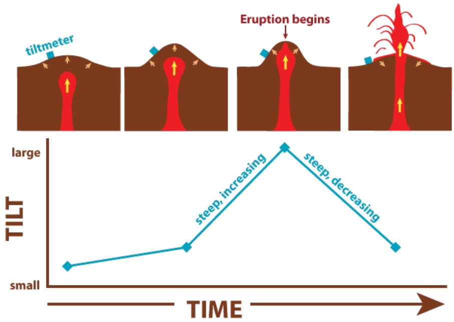

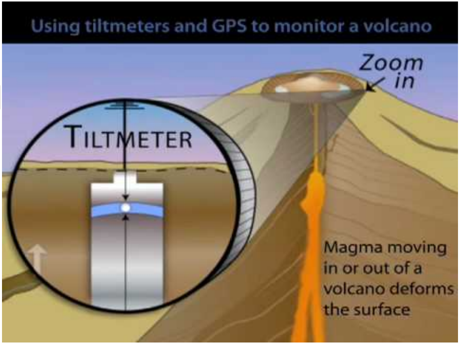

Mount St. Helens Science & Learning Center; Iris

Tiltmeters: Products - time series

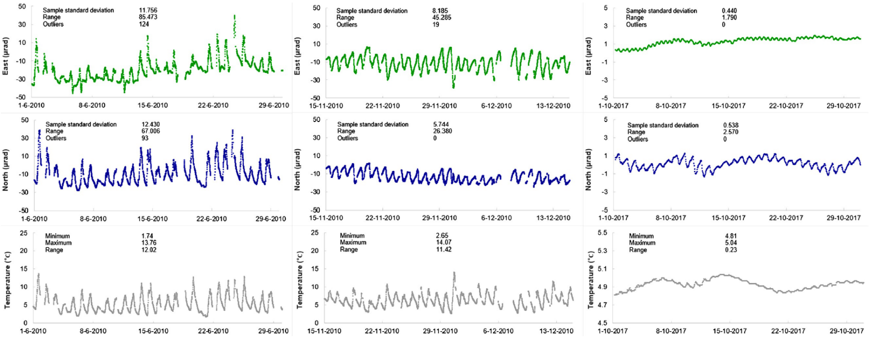

Fig. 8 Time series for tiltmeter SOSO, monitoring Sotara volcano (see Alpala et al., 2017). Left column: tiltmeter installed at the surface, fixed with expansion screws and epoxy cement (Fig. 7, left column). Center column: tiltmeter installed at the surface, fastened to a polished rock surface with screws only. Right: tiltmeter installed below the surface, fastened to a polished rock surface only with screws. The upper row corresponds to the slope in the East component, the middle row to the slope in the North component, and the bottom row to temperature.

Battaglia et al., 2019

Gravity - space based

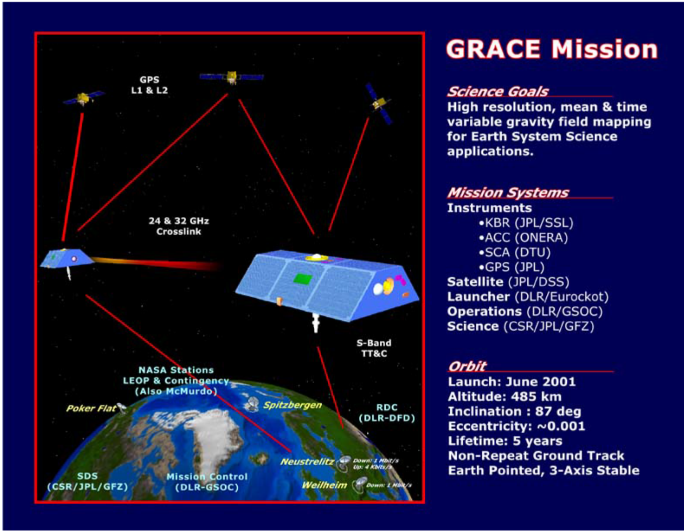

courtesy: Geoscience Australia, http://www.ga.gov.au/scientific-topics/positioning-navigation/geodesy/geodetic-techniques/interferometric-synthetic-aperture-radar

Gravity - space based: product

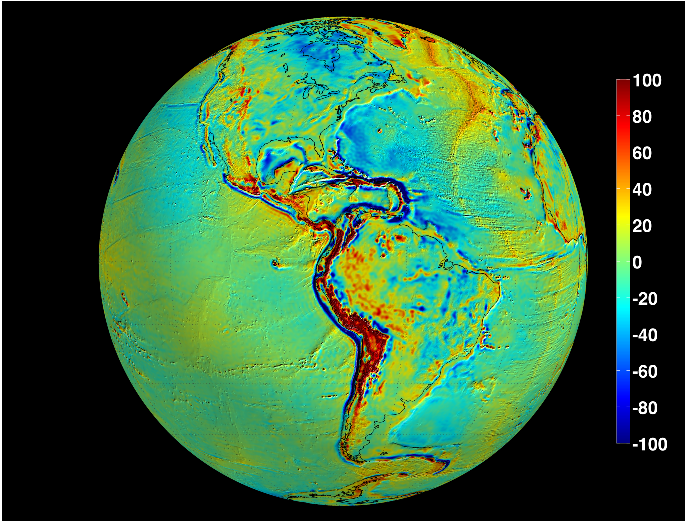

courtesy: NASA-JPL

Gravity - ground-based

Fig. 30 Set up of a gravity benchmark at Mount St Helens. Note the drilled leg holes for the Scintrex CG-5 tripod Photo courtesy of M. Poland, US Geological Survey.

Battaglia et al., 2019

Gravity - ground-based: product

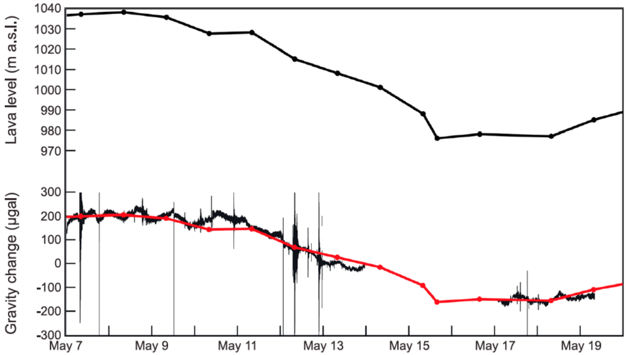

Figure 7. Comparison between lava level (upper plot) and gravity (black curve in lower plot) spanning the May 2015 draining of Kīlauea's summit lava lake. Using the model of *Carbone et al.* [2013], a lava density of ~1400 kg/m^3 is necessary to fit the gravity change based on the constraints provided by the change in lava level (red curve).

Poland and Carbone, 2016

Electronic Distance Measurement (EDM) 1/4

http://volcano.si.edu/Photos/full/035031.jpg

Electronic Distance Measurement (EDM) 2/4

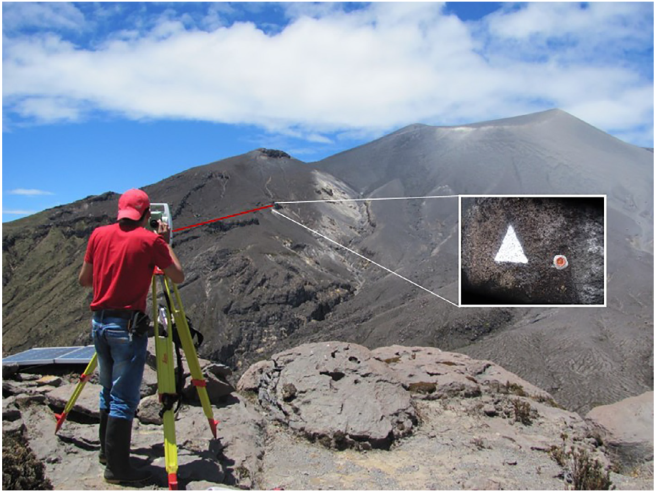

Fig. 1 Using the EDM in the field: measurement of the baseline between a base station and the target reflector installed on the flank of the volcanic edifice—Puracé Volcano (Colombia) using a total station. A total station is an electronic theodolite integrated with EDM and an on-board computer to collect data and perform calculations.

Battaglia et al., 2019

Electronic Distance Measurement (EDM) 3/4

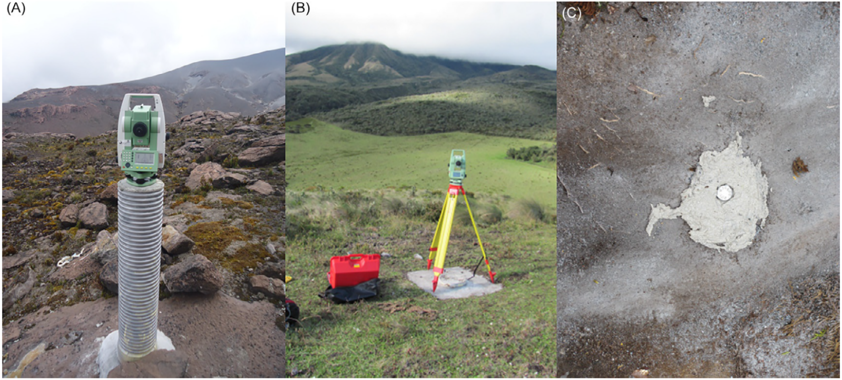

Fig. 2 Different EDM base stations: (A) Concrete column; (B) Concrete baseplate; (C) Small plate or screw in stainless steel.

Battaglia et al., 2019

Electronic Distance Measurement (EDM) 4/4

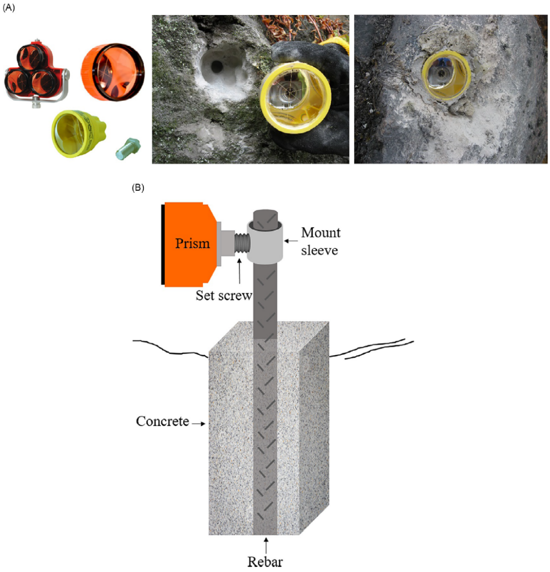

Battaglia et al., 2019

Fig. 3 (A) *Left*: Reflecting prisms for EDM measurements. *Center and Right*: Fixing the prism to the stable outcrop with epoxy cement, in the images the coupling of these in rock is observed. (B) Mounting sleeve attached to anchor rod installed in unconsolidated ground (After Ewert and Swanson, 1992).

Laser Scanning

UNAVCO

Laser Scanning

UNAVCO

Laser Scanning: Product - point cloud

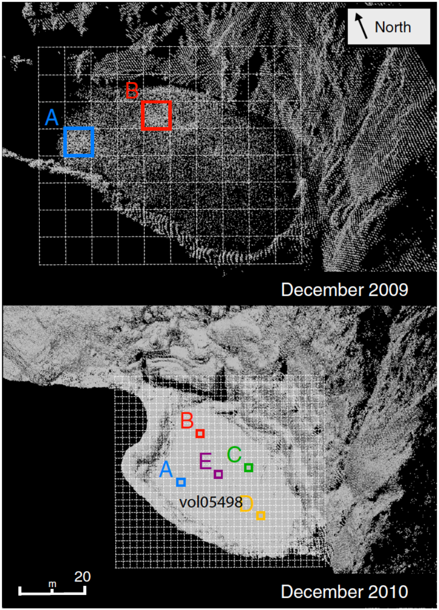

Jones et al., 2015

Laser Scanning: Product - time series

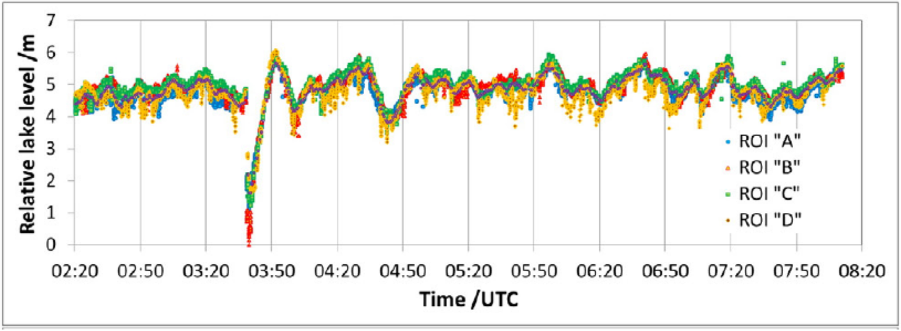

Jones et al., 2015

Structure from Motion

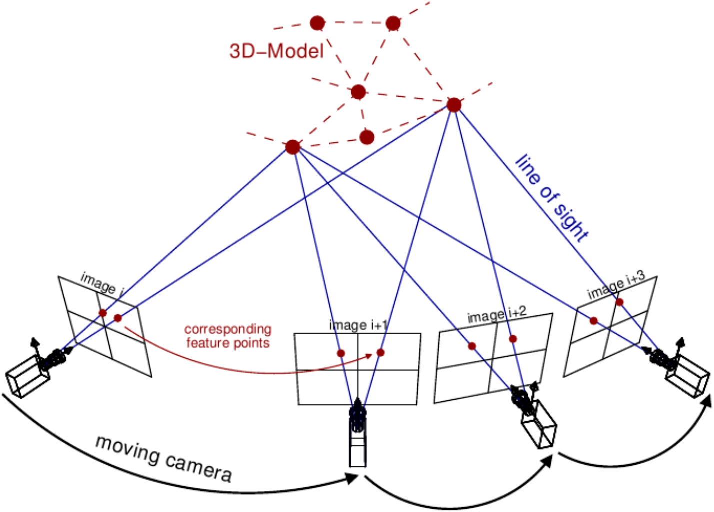

source: Theia.sfm.org 2016

Structure from Motion

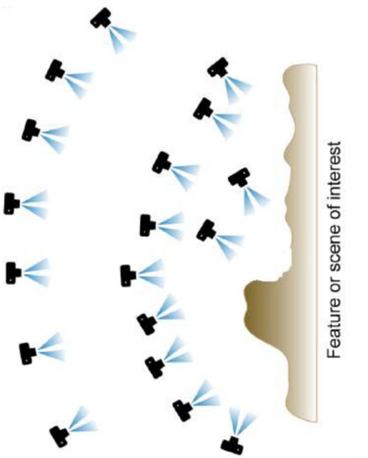

Figure 1: Example of imagery acquisition. Structure from Motion photogrammetry requires multiple photographs with large overlap collected from different positions and directions.

source: Micheletti et al., 2015,Geomorphological Techniques, Chap. 2, Sec. 2.2

Structure from Motion

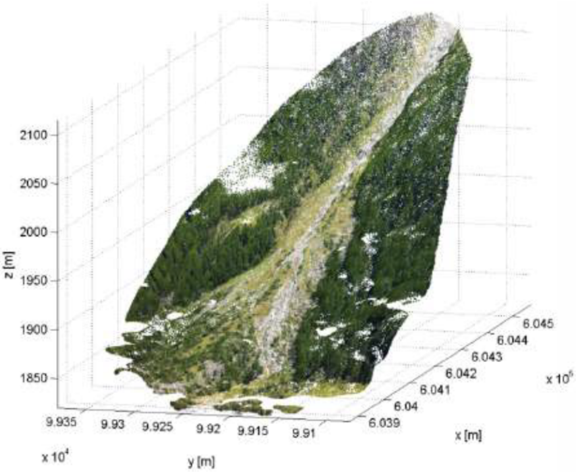

Figure 5: Alluvial fan point cloud generated using smartphone imagery and 123D Catch (Micheletti et al., 2014).

Structure from Motion: Eelriver

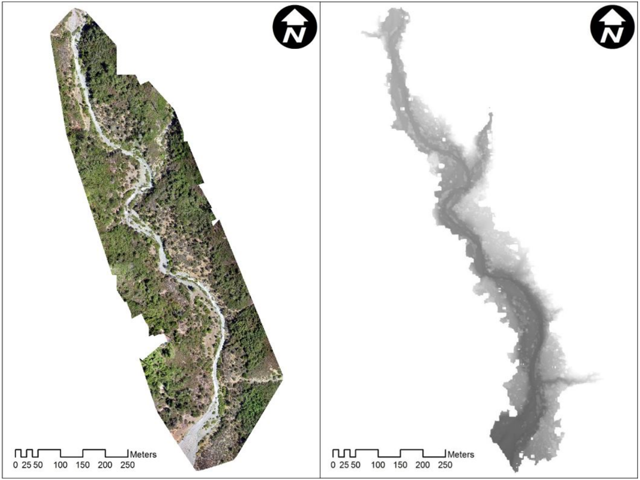

source: http://gsp.humboldt.edu/OLM/Courses/GSP_216_Online/lesson8-2/SfM.html